DesignCon 2012

Practical methodology for analyzing the effect of conductor roughness on signal losses and dispersion in interconnects

Yuriy Shlepnev, Simberian Inc.
shlepnev@simberian.com, +1-702-876-2882

Chudy Nwachukwu, Isola Group
Chudy.Nwachukwu@isola-group.com, +1-480-812-2564

Abstract

In-depth understanding of signal propagation in PCB traces and packaging interconnects has become critical for SI modeling as communication speeds move into 8-40 Gb/s data rates. Despite multiple publications discussing the effects of conductor roughness, a practical analysis of rough interconnects is yet to be proposed. This paper presents useful methodology in characterizing conductor roughness up to 50 GHz. We first identify the dielectric properties of the substrate using test fixtures designed with a smooth copper conductor. Next, we identify the parameters of a proposed roughness model for different types of copper foil. Ultimately, we demonstrate and explain how the capacitive effects of roughness increases interconnect group delay and decreases characteristic impedance.

Takeaway from the paper and presentation:
1) Understanding the advantages and disadvantages of existing roughness characterization methodologies;
2) New simple and universal correction coefficient to account for additional loss and dispersion due to skin effect on rough surfaces;
3) Understanding capacitive effect of roughness due to sharp peaks on conductor surface;
4) Unified methodology to build heuristic roughness models for practical applications.

Author(s) Biography

Yuriy Shlepnev is President and Founder of Simberian Inc., where he develops Simbeor electromagnetic signal integrity software. He received M.S. degree in radio engineering from Novosibirsk State Technical University in 1983, and the Ph.D. degree in computational electromagnetics from Siberian State University of Telecommunications and Informatics in 1990. He was principal developer of electromagnetic simulator for Eagleware Corporation and leading developer of electromagnetic software for simulation of signal and power distribution networks at Mentor Graphics. The results of his research are published in multiple papers and conference proceedings.

Chudy Nwachukwu is a Signal Integrity and Application Development Engineer at Isola Group, responsible for designing test vehicles and engineering applications to meet the requirements of OEMs in the high speed digital market. He completed his MSEE at Saint Cloud State University, Saint Cloud MN in 2009 and published his graduate Thesis on Design optimization of components in High Speed PCBs. He previously worked for Force10 Networks in San Jose, CA specializing in 3D EM simulations and signal integrity analysis of line card and backplane channels.

1. Introduction

During the manufacturing process of printed circuit boards (PCBs), copper foils are treated to increase surface roughness and improve adhesion to dielectrics in order to avoid delamination. The use of varying roughness profiles depends on the performance specification of the PCB package, which include but are not limited to improved etching capabilities, higher peel strength and improved signal quality. Appropriate electrical modeling of conductor roughness on such boards is important for accurate prediction of signal degradation effects discussed in [4]-[8], [10], [13]. Conductor roughness has been shown in [19] to affect dissipation factor at higher frequencies and also the effective dielectric constant of the adjoining resin-system at all frequencies. A systematic low-cost characterization of conductor roughness is a must for accurate signal integrity analysis in interconnects with data rates from 6 to 100 Gbps. **A practical methodology for electrical characterization of roughness effect for analysis of digital and microwave signal propagation in rough PCB and packaging interconnects is the subject of this paper.**

There are multiple methods suggested for modelling the conductor roughness effect. One of the first numerical investigations of the roughness effect was done by Morgan in [1] for simplified surfaces with triangular and rectangular grooves. The results of [1] were fitted by authors of [2] and later published in [3]. This model is widely known as Hammerstad's Correction Coefficient (HCC) and was successfully used for analysis of microwave circuits and recently for PCB interconnects as shown in [4] and [5]. However, the reports on the model applicability for PCB interconnects are shown to be controversial in [6]-[8]. This is mainly because the maximal increase in attenuation due to conductor roughness is limited to a maximum factor of 2 for the traditional HCC. Still, authors of [4]-[6] demonstrated that the model can provide an acceptable degree of accuracy for some types of copper surfaces.

There have been multiple attempts to derive alternative roughness models based on the rough surface power absorption correction coefficients as descried in [6], [7], [9] - [12]. A Hemispherical approximation of rough surfaces was used in [6] to derive the correction coefficient. The "Snowball" model was introduced by Paul Huray in [7] to derive a correction coefficient. Another correction coefficient was introduced by Sandstroem in [9] and validated experimentally in [10]. A correction coefficient known as the power absorption enhancement function based on the power spectral density of the rough surface was introduced in [11] and [12].. In practice, **all roughness correction coefficients were validated with experiments, but still exhibit one common characteristic - it is difficult to define the model parameters for any particular case.** Measurement results obtained using expensive equipment are typically required to define parameters for a particular model. However, only the RMS peak-to-valley value (Rq) is required for the HCC model. That value is typically available from the copper or laminate manufacturer. The restrictive factor of 2 discussed earlier can be removed by introducing the roughness factor coefficient as is done in this paper.

An alternative approach to utilizing the correction coefficient is the application of equivalent generalized impedance boundary conditions as suggested in [15] and [20]. Three-dimensional electromagnetic approximation of rough surfaces can be directly used to simulate the effect of roughness as it is done in [13], [14], [15] and [16].. However, the major problem with the application of equivalent boundary conditions and 2D/3D

surface analysis is that the error of the surface approximation relative to the actual rough surface is unknown. The rough surface is technically fractal in nature as explained in [17] and thus, cannot be approximated by simple geometric shapes. The pictures shown in [7] illustrate this point. The **authors of [6] and [7] also pointed out that measurements with a profilometer or from micro-photographs of cross-sections may be misleading in predicting the effect of the roughness topography.** It has been shown that the profilometer data or micro-photography may not provide sufficient resolution to capture all the peculiarities of the rough surface.

In this paper, we propose a practical procedure for identifying parameters for any roughness correction coefficient without the complexities required in investigating the micro-structure of the conductor surface. The idea is to avoid the microscopic investigation of the conductor surface and use a roughness correction coefficient as a macro-model with parameters defined by matching simulated and modelled generalized modal S-parameters. The procedure was first proposed for identification of dielectrics in [24], and subsequently generalized for any PCB/packaging material identification in [25]. Subsequently, the method was successfully used for identification of roughness parameters in [19] and parameters of nickel plating in [26]. In this paper, the procedure is illustrated with the identification of parameters for three different roughness correction coefficients (Simbeor model, modified Hammerstad model, and Huray's snowball model). We begin with an experimental observation of the roughness effect on insertion loss and group delay in PCB interconnects designed with standard and low-profile copper roughness. A test board was manufactured with two different grades of copper (RTF and VLP) on each half of the board. Micro-strip and strip line segments of two different lengths were placed on the board to measure generalized modal S-parameters (GMS-parameters) for the roughness parameter extraction.

First, we show that modeling interconnects with dielectric parameters defined by the Bereskin method with smooth copper predicts lower insertion loss for both foils and also lower group delay. Next, we build an electromagnetic model of interconnects with the novel roughness model. A roughness correction coefficient is used for the local adjustment of the differential surface impedance operator constructed for the interconnect conductor with Trefftz finite elements. The model is causal and takes into account both the resistive and inductive components of skin-effect on a rough surface. To build a universal roughness model that can be reused in different software applications, we extend the Hammerstad correction coefficient model to simulate cases with a possible increase in attenuation smaller than or larger than 2 (limit of the original widely used correction coefficient). The proposed model can be used with any numerical technique for the analysis of lines with lossy conductors. It can be also used with any derived roughness correction coefficient such as Huray's snowball model. We will show how to identify the parameters of each without the expensive investigation of rough surface micro-structure, and then compare the results generated from each model.

In addition to a slight increase in internal inductance and an increase in attenuation due to increased absorption by the rough surface (skin-effect), a substantial increase in the conductor capacitance is also observed as shown in [18] and [19]. This is explained by accounting for additional charges on the peaks of the rough conductor surface profile. This effect is typically mitigated in analysis by adjusting the dielectric constant of the substrate. However any changes in trace width may require

an additional adjustment of the effective dielectric constant. We propose an alternative approach by building a numerical model with short spiky "needles" evenly distributed on a strip or metallization plane surface (singular surface). The parameters of this hybrid heuristic model can be extracted with the GMS-parameters technique similar to the identification of dielectric parameters. **The suggested roughness characterization procedure is practical and can provide a reliable prediction of interconnect behavior for a particular laminate manufacturing process.** We will show that the suggested approach is acceptable for analysis of interconnects within some variation of trace widths at frequencies from DC to 50 GHz or with data rates from 8-40 Gbps.

2. Test board design and measurements

To investigate the effect of roughness, a PCB with 8 layer stackup has been designed and manufactured. The board in a micro-probe station is shown in Fig. 1. The board stackup is shown in Fig.2. It has two microstrip layers (top and bottom) and 2 strip-line layers (L3, and L6). Two different copper foils and two different dielectrics are used to manufacture the board.
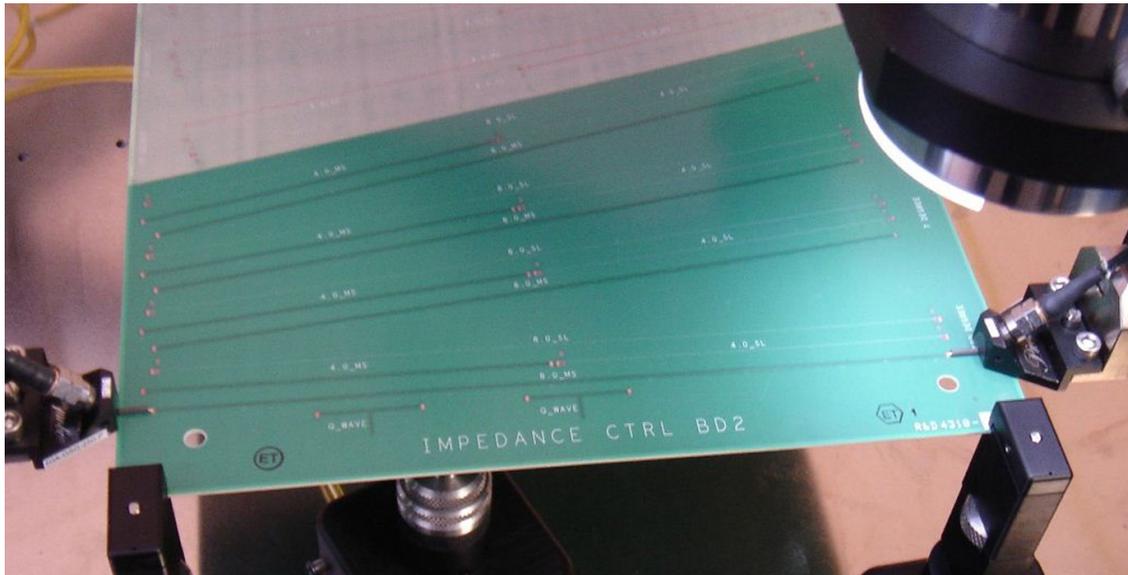

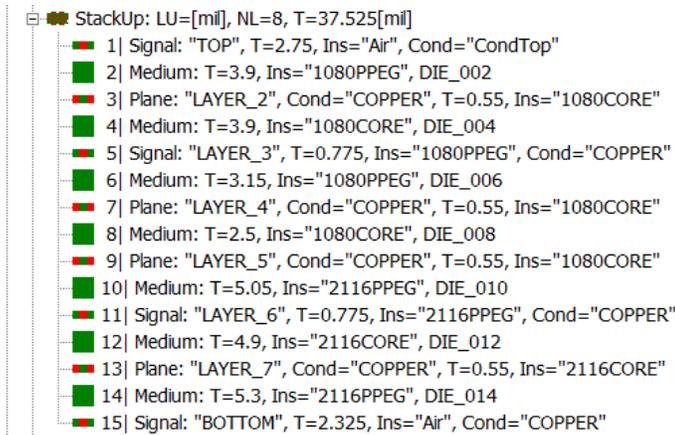*Fig. 1. Test board in the micro-probe station.*

```
StackUp: LU=[mil], NL=8, T=37.525[mil]
   1| Signal: "TOP", T=2.75, Ins="Air", Cond="CondTop"
   2| Medium: T=3.9, Ins="1080PPEG", DIE_002
   3| Plane: "LAYER_2", Cond="COPPER", T=0.55, Ins="1080CORE"
   4| Medium: T=3.9, Ins="1080CORE", DIE_004
   5| Signal: "LAYER_3", T=0.775, Ins="1080PPEG", Cond="COPPER"
   6| Medium: T=3.15, Ins="1080PPEG", DIE_006
   7| Plane: "LAYER_4", Cond="COPPER", T=0.55, Ins="1080CORE"
   8| Medium: T=2.5, Ins="1080CORE", DIE_008
   9| Plane: "LAYER_5", Cond="COPPER", T=0.55, Ins="1080CORE"
  10| Medium: T=5.05, Ins="2116PPEG", DIE_010
  11| Signal: "LAYER_6", T=0.775, Ins="2116PPEG", Cond="COPPER"
  12| Medium: T=4.9, Ins="2116CORE", DIE_012
  13| Plane: "LAYER_7", Cond="COPPER", T=0.55, Ins="2116CORE"
  14| Medium: T=5.3, Ins="2116PPEG", DIE_014
  15| Signal: "BOTTOM", T=2.325, Ins="Air", Cond="COPPER"
```

Fig. 2. Test board stackup.

The dielectric constant (Dk) and loss tangent or dissipation factor (Df) for both dielectrics were identified in a separate experiment with accurate Bereskin's strip-line method [21] using smooth copper. The results are Dk=3.0 and Df=0.003 for I-Tera 1080 laminate (both core and prepreg) and Dk=3.3 and Df=0.0034 for the I-Tera 2116 laminate. The values are measured at 2, 5 and 10 GHz. Note that it is normal to have almost constant dielectric constant and loss tangent in this frequency band for these types of dielectrics with very low polarization losses. The Wideband Debye (also known as Djordjevic-Sarkar) model presented in [22] predicts such behaviour. Thus, these values will be used for all computations in this paper. The values of Dk and Df at 2 GHz are used to define the wideband Debye model.

The test structures on this board are 4 and 8 inch straight microstrip and strip lines with transitions to probing pads on the surface of the board. Microstrip lines in the top layer are 8.9 mil wide strips made of very rough standard RTF copper foil on I-Tera 1080 prepreg laminate without solder mask. To improve accuracy of experiment, the strip widths as well as the dielectric layer thicknesses are measured after fabrication from micro-photographs of the board cross-sections as shown in Fig. 3-4. Strip lines in layer L3 are 4.1 mil wide strips made of RTF copper foil and sandwiched between 1080 core and prepreg laminates. Strip lines in layer L6 are 5.7 mil wide strips made of low roughness profile VLP copper foil between I-Tera 2116 core and prepreg laminates. Microstrip lines in the bottom layer are 12.9 mil wide strips made of VLP copper foil on 2116 prepreg laminate.
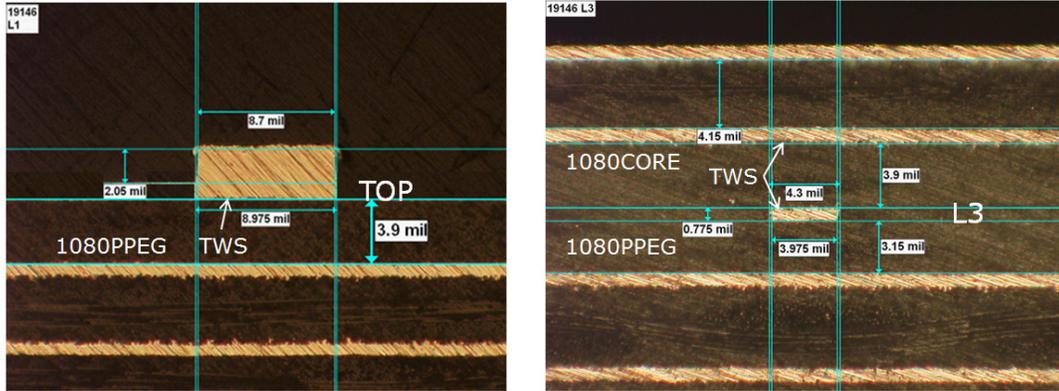
Fig. 3. Micro-photographs of cross-sections and dimensions for top microstrip (left) and strip line in layer L3 (right).
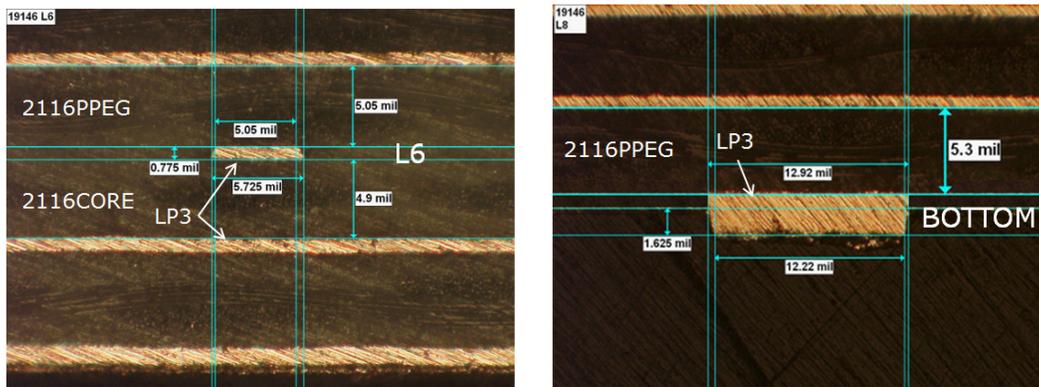

Fig. 4. Micro-photographs of cross-sections and dimensions for bottom microstrip (right) and strip line in layer L6 (left).

S-parameters were measured for all transmission line segments with an Agilent VNA. The reflection loss was below -20 dB up to 20 GHz and below -10 dB up to 50 GHz as shown on the plots in Fig. 5 and 6 for the top microstrip and L3 strip line segments. The data obtained were passive, but had substantial reciprocity and causality violations at higher frequencies and the quality was questionable. Thus, the data quality was estimated with the rational macro-models in Simbeor Touchstone Analyser [23] and considered to be acceptable for further analysis (no improvement was necessary).
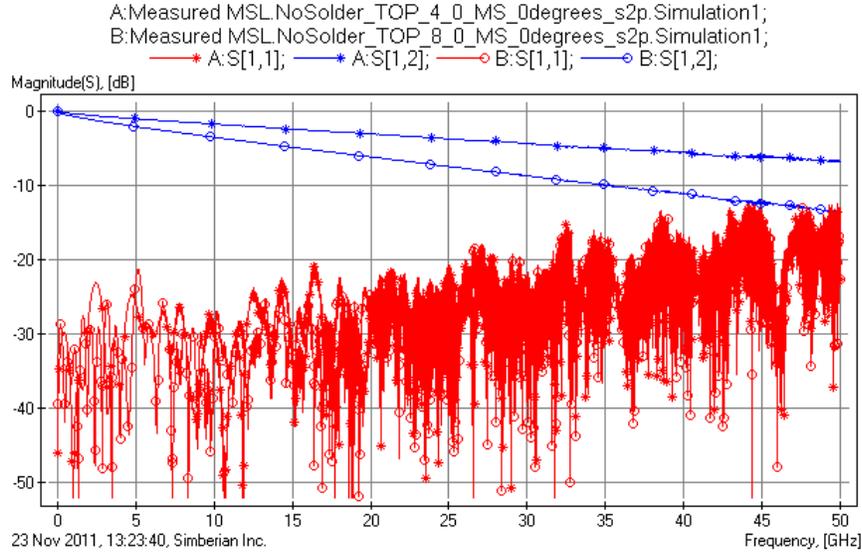
Fig. 5. Insertion loss (blue) and reflection loss (red) for 4-inch (stars) and 8-inch (circles) segments of microstrip line in the top layer (L1, RTF, 1080). Data quality is acceptable (QM > 90%). Data provided by INAOE.
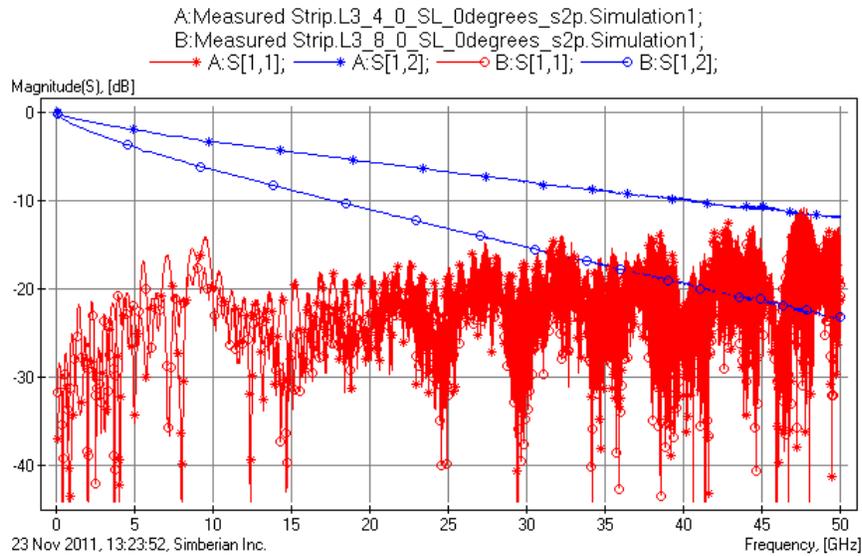

Fig. 6. Insertion loss (blue) and reflection loss (red) for 4-inch (stars) and 8-inch (circles) segments of strip line in layer L3 (RTF, 1080). Data quality is acceptable (QM>90%). Data provided by INAOE.

The measured data had low reflection and no resonances in the insertion loss. However, the direct use of the transmission coefficients (insertion loss and phase or group delay) for material property identification may have introduced uncertainties due to the non-zero reflection losses, especially at frequencies above 15-20 GHz. Thus, **pairs of lines are used to extract the reflection-less generalized modal S-parameters (GMS-parameters) of 4-inch line segments following the procedure described in [24], [25] (shown in Fig. 7 and 8)**.
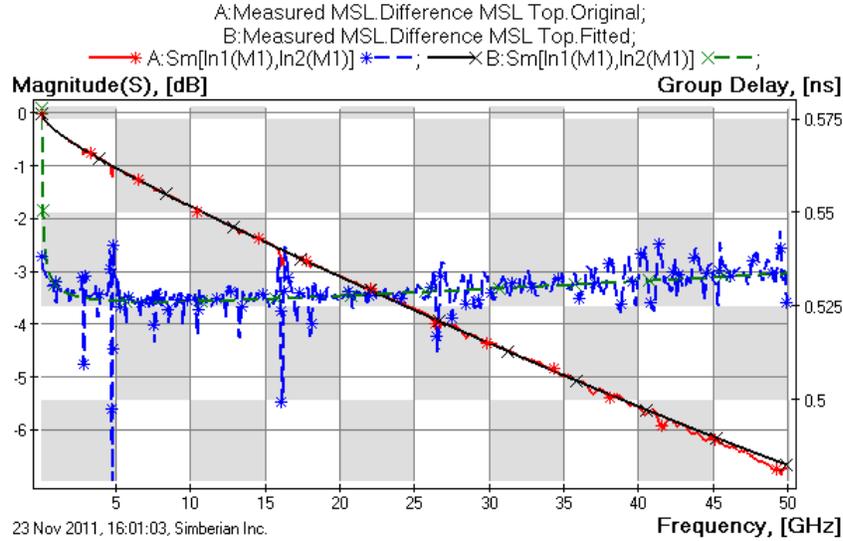
Fig. 7. Generalized modal insertion loss (red and black lines, left axis) and group delay (blue and green lines, right axis) for 4-inch segment of microstrip line in top layer (RTF, 1080). Original data – red and blue line, fitted results – black and green lines.
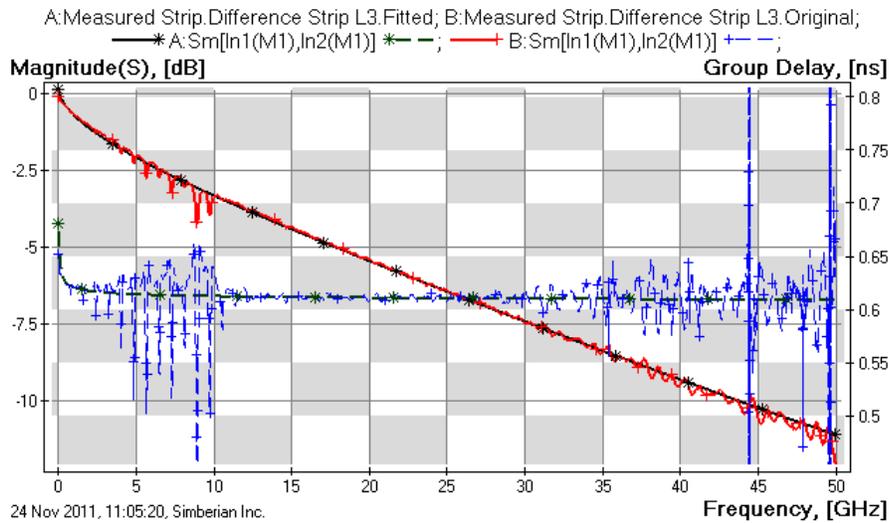

Fig. 8. Generalized modal insertion loss (red and black lines, left axis) and group delay (blue and green lines, right axis) for 4-inch segment of strip line in layer L3 (RTF, 1080). Original data – red and blue lines, fitted results – black and green lines.

GMS-parameters were additionally fitted with square root of frequency plus a third order polynomial function to minimize measurement and noise caused by the non-identical nature of the test fixtures (RMS fitting errors in magnitudes are less than 0.005, in phases less than 1.5 deg.). The non-fitted and fitted GMS transmission coefficients for the top microstrip and strip line in layer L3 are plotted for comparison in Fig. 7 and 8. We observed that the group delay in the microstrip line increases at frequencies above 5 GHz due to high-frequency dispersion caused by the inhomogeneous dielectric (field concentration in dielectric at high frequencies). **This effect can be captured only with full-wave electromagnetic analysis.** Group delay for the strip line goes slightly down due to relative homogeneity of dielectric and slight decline of dielectric constant that can

be predicted by the wideband Debye model. All these effects have to be considered and are appropriately accounted for during the material parameters identification process. The group delay is estimated here with 7-th order smoothing differentiators. Non-fitted group delay exhibit relatively large variations that are not optimal for parameter identification due to the different types of artefacts in test fixtures (physical non-identities) and noise. However, group delay computed from fitted phase data is smooth and suitable for the identification. Alternatively, the phase of the original GMS transmission can be used for the material model identification – the fitted phase graph is practically overlayed on the original phase data as shown in Fig. 9 (RMS error is 1.2 deg.).
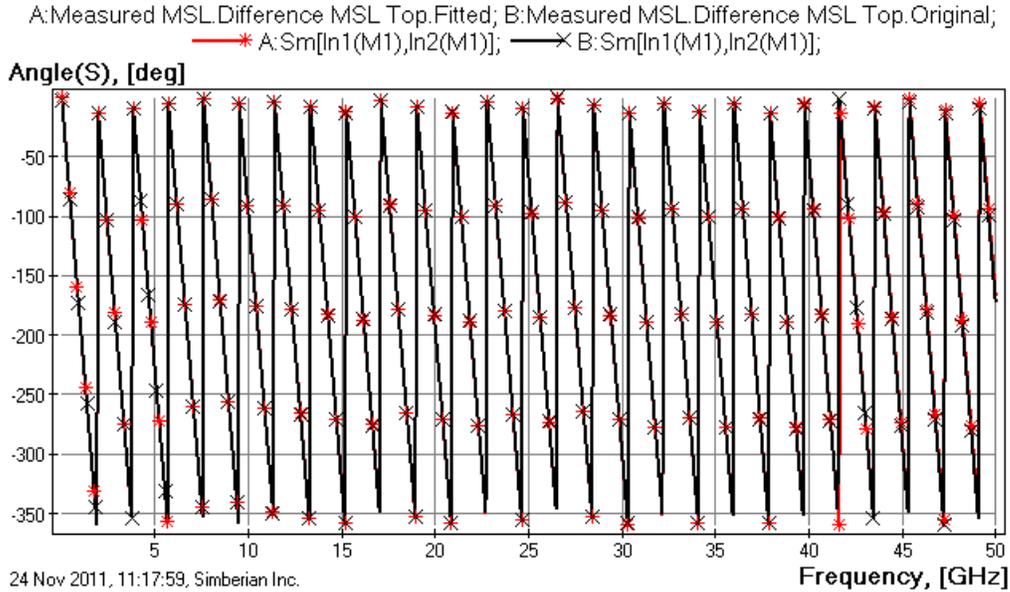

Fig. 9. Generalized modal transmission phase for 4-inch segment of microstrip line in top layer (RTF, 1080). Original data – red stars, fitted results – black crosses.

At this stage, measured reflection-less GMS-parameters for four 4-inch segments of microstrip and strip line structures (in layers top, bottom, L3 and L6), have been prepared to verify the dielectric model and to identify parameters of the conductor roughness. Here we assume that the dielectric properties are known. Ideally, we would need a separate experiment to ensure that the broad-band dielectric models worked as expected. In addition, GMS-parameters for line segments made of smooth copper on the same board would be ideal for separate identification of dielectric properties over the extremely wide frequency band (from 10 MHz to 50 GHz in this particular case).

3. Preliminary analysis of roughness effect

Now we proceed to compute GMS-parameters of 4-inch line segments with the dielectric parameters defined by Bereskin's method. We perform this computation first assuming that all conductors have smooth surfaces (no roughness effect included). We use the causal Djordjevic-Sarkar model [23] to characterize all dielectrics with parameters defined at 2 GHz. The results of this preliminary analysis are plotted with

circles in Fig. 10 and Fig. 11. The measured GMS-parameters are plotted on the same graphs with stars.
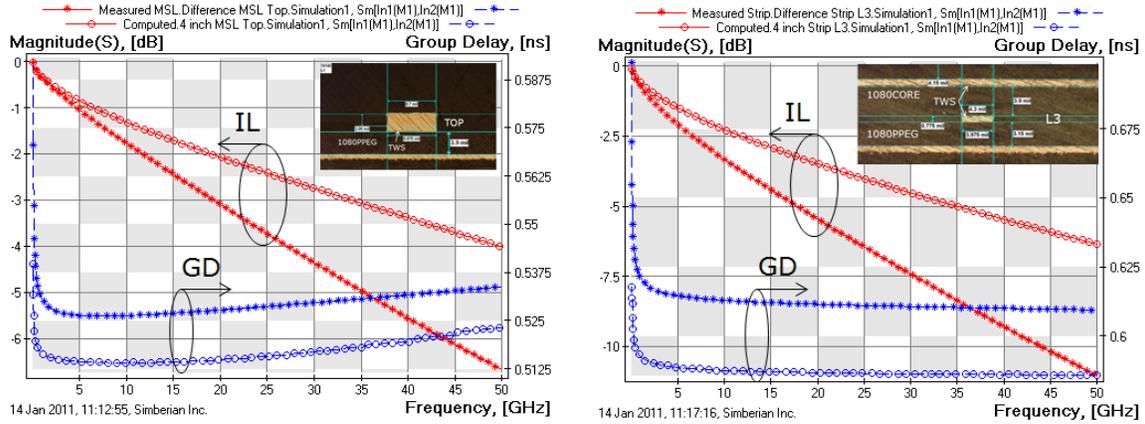

Fig. 10. Measured (stars) and preliminary computed (circles) generalized modal insertion loss (IL, red curves) and group delay (GD, blue curves) of 4 inch microstrip line in top layer (left plot) and strip line in layer L3 (right plot). Foil RTF, laminate 1080.
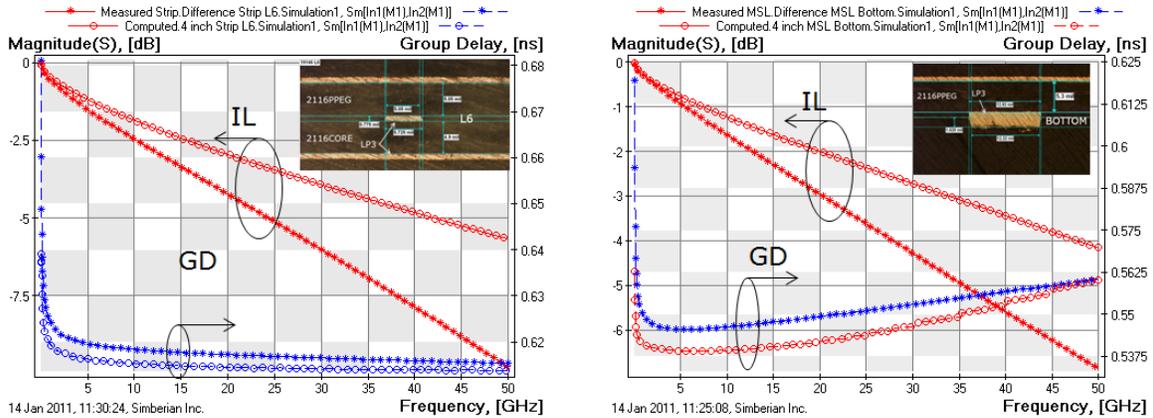

Fig. 11. Measured (stars) and preliminary computed (circles) generalized modal insertion loss (IL, red curves) and group delay (GD, blue curves) of 4 inch strip line in layer L6 (left plot) and microstrip line in bottom layer (right plot). Foil VLP, laminate 2116.

We observed a substantial difference in the insertion loss for all four types of transmission lines even with the low-profile roughness foil. Group delays for the microstrip line in the top layer and for the strip line in layer L3 (made of rough RTF foil and 1080 laminate) were also substantially different from the measured data as we can see from Fig. 10. In the case of the microstrip line on the top layer, the relative difference in group delay was slightly smaller than in the case of the strip line in layer L3. Computed group delays for the microstrip line in the bottom layer and for the strip line in layer L6 (VLP foil and 2116 laminate) were much closer to the measured data as we can see in Fig. 11. To match the modelled and measured group delays for all four types of lines, we adjusted the dielectric constants as follows: from 3 to 3.15 for 1080 prepreg and to 3.35 for 1080 core, from 3.3 to 3.36 for 2116 prepreg and to 3.25 for 2116 core. The adjustment for the 2116 laminate is within the 5% limit expected for such

material. However, the adjustment for the 1080 core laminate exceeds 10%. A possible explanation is the sparse weave fibres in the 1080 laminate affecting the observed Dk which is larger due to glass-fibre effect on the stripline discussed in [32]. However, the board had traces running at 7, 10 and 15 degrees to the fibres and all cases showed consistent increase in the effective dielectric constant as shown in Fig. 12.
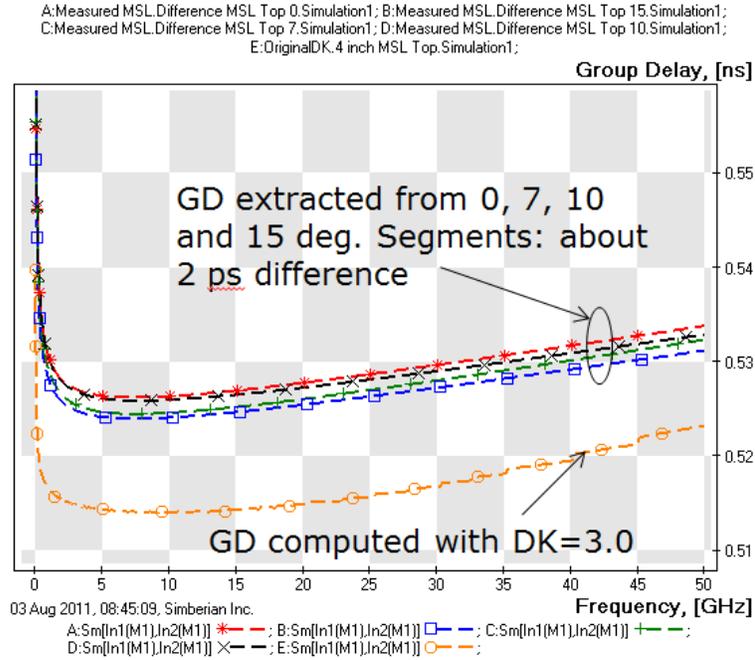

Fig. 12. Generalized modal group delay (GD) of 4 inch microstrip line in top layer extracted for 0, 7, 10 and 15 deg. traces (computed from fitted phase). GD computed with Dk=3.0 is shown by yellow line (circles) and consistently lower.

Another possible explanation is that the group delay or effective dielectric constant increases due to the roughness effect as noted in [8] and [13]. Authors of [8] suggested that roughness increases the line inductance. However, the observed group delay is larger even at very low frequencies where there is no skin-effect, and current is uniformly distributed across the conductor. Such large increases in group delay and effective dielectric constant would require at least a 10% increase in observed total inductance per unit length. The internal inductance should be about twice that of theoretically predicted value for a solid copper conductor with the same cross-section at DC. In addition, the effect of increased inductance should be also visible as an increase of the characteristic impedance. Theoretically, an increase of the dielectric constant, and hence the capacitance should lead to a decrease of characteristic impedance. This is exactly what was observed in this case as illustrated in Fig. 13.
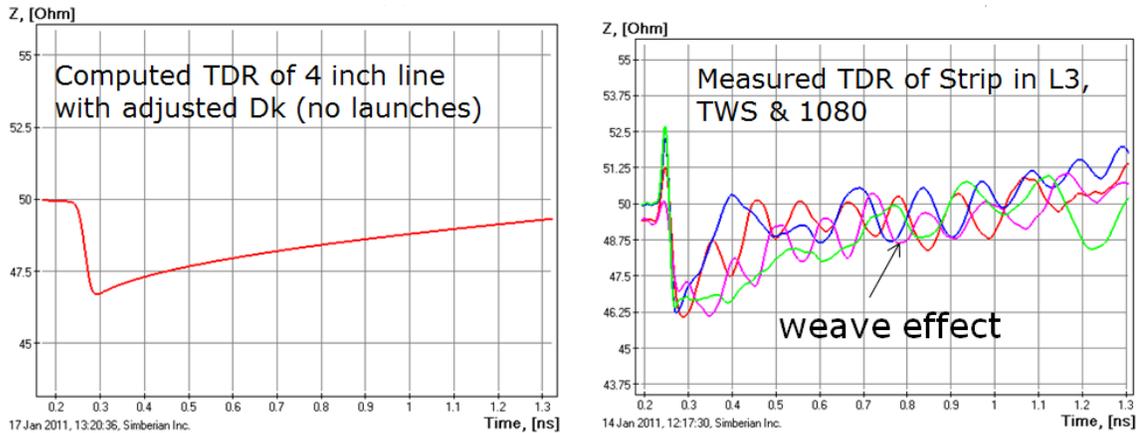
Fig. 13. Computed TDR plot for a 4-inch strip line in layer L3 with adjusted Dk (left plot) and measured TDR (computed from measured S-parameters) for all strip line structures in layer L3.

Characteristic impedance computed with the increased dielectric constant was in good agreement with impedance data from TDR. The difference would be about 10% if the roughness increased the inductance. We did not observe such a difference. Thus, **the most probable explanation of the phenomenon is simply an increase of capacitance due to the spikes on the rough conductor surface.** This increase in capacitance can be especially large for thin laminates. Note, that the capacitive effect of roughness was reported, explained and even modelled for IC applications in [18]. On our test board, maximal peak-to-valley roughness value measured with profilometer was 11.3 μm for RTF and only 3.1 μm for VLP foil. The electrical field may be nearly singular on the sharp surface peaks of the strip similar to the singularities at the strip edges. The top layer microstrip line had only one very rough surface (bottom side of the strip) and the capacitance increase was only about 5%. The strip line on layer L3 has two rough surfaces (top side of the strip and plane above the strip), and corresponding capacitance increased about 10%. This is clear evidence of the capacitive effect of conductor roughness and it explains the large adjustment for dielectric constant on laminates facing the rough side of the conductor. **Additional capacitance can be simulated either with the adjustment of dielectric constants or with an array of small spikes on the conductor surface as will be shown later in this paper.**

Technically, we can adjust the loss tangent of the dielectric and match the insertion loss in the same way as we did with the group delay. We performed this experiment and noticed that multi-pole Debye model discussed in [23] has to be used to achieve good agreement both in the insertion loss and group delay. Unfortunately, as noted in [4], the accuracy of such a model may be specific only to a given trace width. Note also that the direct separation of losses detailed in [10] might seem an appealing idea, but it may be difficult for such low-loss dielectrics. As we can see from Fig. 10 and 11, the losses due to roughness are substantial and grow with frequency, faster than the square root of frequency – roughness may contribute to the linear term. These dielectric losses may also not be proportional to frequency due to a slight increase of loss tangent with frequency. Thus, the natural next step is to build a computational model taking rough conductor surfaces into account and matching the model to the measured GMS-parameters of line segments.

4. Model for transmission line with rough conductor

To improve the analysis of the line segment, we first build an electromagnetic model of the transmission line segment with a rough conductor surface. We use a hybrid technique based on the method of lines extended to planar 3D structures introduced in [27] and combined with the Trefftz finite elements discussed in [28] to simulate the interior of the conductor with a rough surface. We first mesh the conductor interior with rectangular Treftz-Nikol'skii elements with one component of electric field along the conductor and two components of magnetic field in the plane of the conductor cross-section as shown in Fig. 14.
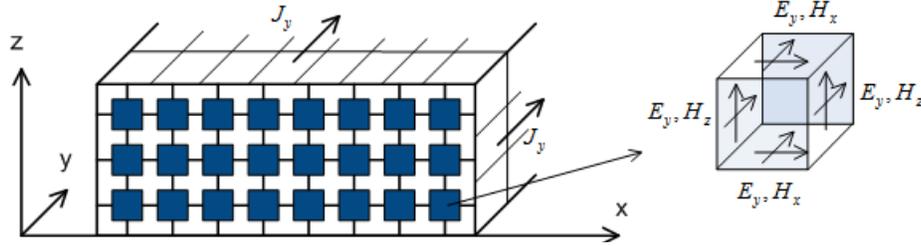

Fig. 14. Trefftz finite element model of the three-layer conductor (elements have different size along the Z-axis).

Trefftz elements are built with the plane-wave solutions of Maxwell's equations in element medium as the intra-element basis functions. The intra-metal element can be described by a differential impedance matrix Z_{el} that relates local voltages (integral of electric field) and surface currents (integral of magnetic field) on the faces of element as follows [28]:

$$Z_{el} = Z_m \cdot \begin{bmatrix} \dfrac{\coth(\Gamma \cdot dz)}{dx} & \dfrac{1}{\Gamma \cdot dx \cdot dz} & \dfrac{\operatorname{csech}(\Gamma \cdot dz)}{dx} & \dfrac{1}{\Gamma \cdot dx \cdot dz} \\ \dfrac{1}{\Gamma \cdot dx \cdot dz} & \dfrac{\coth(\Gamma \cdot dx)}{dz} & \dfrac{1}{\Gamma \cdot dx \cdot dz} & \dfrac{\operatorname{csech}(\Gamma \cdot dx)}{dz} \\ \dfrac{\operatorname{csech}(\Gamma \cdot dz)}{dx} & \dfrac{1}{\Gamma \cdot dx \cdot dz} & \dfrac{\coth(\Gamma \cdot dz)}{dx} & \dfrac{1}{\Gamma \cdot dx \cdot dz} \\ \dfrac{1}{\Gamma \cdot dx \cdot dz} & \dfrac{\operatorname{csech}(\Gamma \cdot dx)}{dz} & \dfrac{1}{\Gamma \cdot dx \cdot dz} & \dfrac{\coth(\Gamma \cdot dx)}{dz} \end{bmatrix} \quad (1)$$

where $\Gamma = (1+i)\dfrac{1}{\delta_s}$ is the intra-metal plane wave propagation constant, $Z_m = \dfrac{\Gamma}{\sigma}$ is the intra-metal plane wave impedance, $\delta_s = \sqrt{\dfrac{2}{2\pi \cdot f \cdot \mu \cdot \sigma}}$ is the skin depth, σ is the metal conductivity, μ is the metal permeability, f is the frequency, and dx, dz are element sizes along the X and Y axes as shown in Fig. 14. The element of Trefftz-Nickol'skii (1) is reciprocal and conservative at all frequencies. In addition, the element matrix (1) has correct low and high-frequency asymptotes. Skin-effect is automatically accounted for in the element formulation - element size can be much larger than the skin depth. In fact, even one element can be considered as a good approximation of a typical strip conductor.

A detailed analysis of the accuracy of Trefftz elements in analysis of conductors is provided in [19].

The impedance matrices Z_{el} of all the elements in the conductor cross-section are simply connected, following the procedure similar to that described in [28]. A conductor impedance matrix Z_{cs} that relates local voltages and surface currents at the surface of the conductor is formed. This procedure of connecting matrices enforces the boundary conditions between two Trefftz elements. The final matrix is a differential surface impedance operator and, by definition, is similar to the admittance operator introduced in [30]. A differential surface impedance matrix is united with the grid Green's function (or matrix) explained in [27], describing multi-layered dielectric and conductive planes and built with the method of lines. With this hybrid technique, we computed admittance parameters for two segments of transmission lines and extracted complex propagation constant Γ_{TL}, characteristic impedance, complex impedance and admittance per unit length following the procedure introduced in [29]. Using the computed Γ_{TL}, the generalized modal S-matrix of the line segment with length dL can be computed as:

$$Sg = \begin{bmatrix} 0 & \exp(-\Gamma_{TL} \cdot dL) \\ \exp(-\Gamma_{TL} \cdot dL) & 0 \end{bmatrix} \quad (2)$$

Matrix Sg is normalized to the complex frequency-dependent characteristic impedance of the line and does not have reflection. In the case of a coupled or multi-conductor line, such a matrix has zero modal transformation terms as shown in [24]. GMS-parameters can also be extracted from measured S-parameters of the two line segments as shown in [24]. Again, it can be done without any knowledge of the characteristic impedance of the lines. The measured GMS-parameters will have exactly zero reflection and mode transformation coefficients. **Matching magnitude and group delay or phase of computed (2) and measured generalized modal transmission coefficients is the simplest possible way to identify the material properties.**

To account for roughness, the conductor surface impedance matrix Z_{cs} can be adjusted to simulate additional losses and the inductance of the rough conductor surface. One approach is to introduce a layer of elements on the surface of the conductor with effective permittivity and permeability as suggested in [15] and [20]. Another possibility is to use a correction coefficient and adjust the cross-section impedance matrix before uniting it with the method of lines Green's operator which describes multilayered media. For that purpose, we first compute correction coefficients and place them in the diagonal elements of matrix K_{sr} and then multiply the conductor impedance matrix with the correction matrix as follows:

$$Z_{cs}^{"} = K_{sr}^{1/2} \cdot Z_{cs} \cdot K_{sr}^{1/2} \quad (3)$$

Matrix K_{sr} has the same dimension as the conductor cross-section impedance matrix Z_{cs}. The correction coefficients may be different for different sides of the strip. For example, if the top and bottom strips have different roughness type or values, the corresponding correction coefficients on diagonal of K_{sr} can be adjusted to account for the differences. This will force current re-distribution in the conductor cross-section and minimizes total conductor losses (though, overall losses will be always larger with the rough conductor surface). Similar surface impedance correction is used here in the

spectral domain to account for roughness of the conductive plane layers. **Any roughness correction coefficient introduced in [3], [6], [7], [9]-[12], [16] can be used in (3) for adjustment of the surface impedance operator.** Both the real and imaginary parts of the surface impedance are adjusted simultaneously. **This implies that not only the resistance, but also the internal conductor inductance is adjusted to account for the roughness.** This is in accordance with Leontovich's surface impedance boundary conditions and with Wheeler's formula in [31] that equates the real and imaginary parts of impedance for conductors with well-developed skin-effect. However, disproportionally large increases in the internal inductance of the conductor as suggested in [8] cannot be predicted by this model. Note that the approach with correction coefficients (3) can be considered as the local version of the total resistance adjustment suggested in [5]. Typically, attenuation is adjusted with a roughness correction coefficient that leads to non-causal results. However, the approach with the total resistance is less accurate because there is no possible way of accounting for roughness on a particular surface in addition to quasi-static approximation (no high-frequency dispersion).

Finally, for a practical illustration of the roughness correction algorithm **we modify Hammerstad correction coefficient [3] as follows**:

$$k_{sr} = 1 + \left(\frac{2}{\pi} \cdot \arctan\left[1.4\left(\frac{\Delta}{\delta_s} \right)^2 \right] \right) \cdot (RF - 1) \ (4)$$

where δ_s is the skin depth defined earlier, Δ is RMS peak-to-valley distance (may be also considered as a parameter to fit), and RF is a new parameter that is called roughness factor ($RF>1$). **RF characterizes the expected maximal increase in conductor losses due to roughness effect.** Obviously, $RF=2$ derives the classical Hammerstad equation [3] with maximal possible increase in conductor loss equal to 2. We denote model (4) as the modified Hammerstad correction coefficient (MHCC).
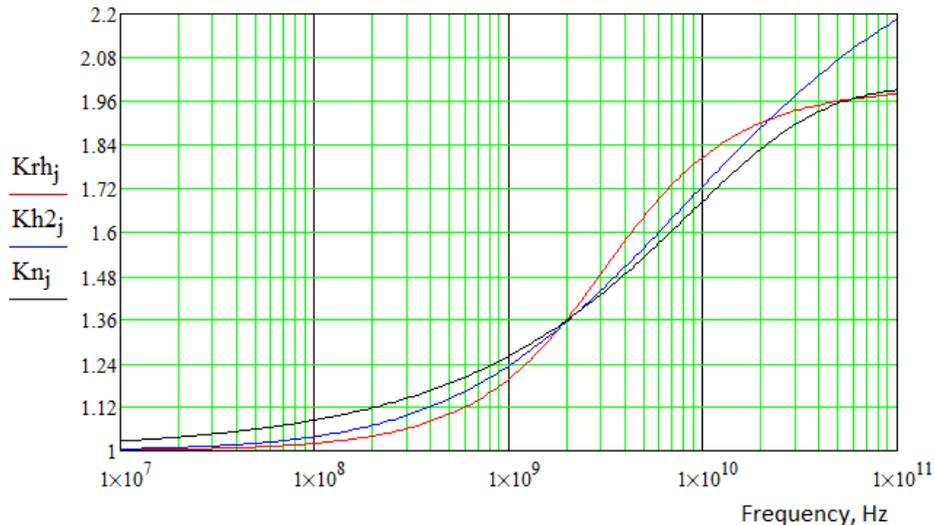

Fig. 15. Comparison of roughness correction coefficients. MHCC model - red line, $\Delta = 1um$ RF=2.0. Huray's snowball model – blue line, sphere radius 0.85um, tile size 11 um, Ns=20. Simbeor model – black line, $\Delta = 1um$ RF=2.0.

16

For further computations we will also use another form of (4) obtained by fitting numerical data for surfaces with triangular profiles implemented in Simbeor software as an alternative to the MHCC. We denote this model as the Simbeor model (first introduced in 2007). For comparison, we will also use roughness correction coefficient derived from Huray's snowball model presented in [7]. All three correction coefficients are plotted in Fig. 15 for comparison – parameters of the models can be adjusted to have a difference within 10%, up to 50 GHz in this particular set of measurements. **Note that all three coefficients are physical – they are based on models that describe increase in conductor surface absorption when skin-effect is developed on a non-flat surface.** In other words, the models describe skin-effect on rough surfaces. The differences are in the approximation of non-flatness or micro-structure of the surface.

The outlined algorithm was first published in [19] and used for analysis of plated rough conductors in [26]. The algorithm for analysis of rough conductors with all three roughness correction coefficients is implemented in the electromagnetic signal integrity software Simbeor 2012 [22] that is used for all computations in this paper.

5. Roughness identification with GMS-parameters

Here we used generalized modal S-parameters (GMS-parameters) for validation and identification of material parameters. **Due to zero reflections, no modal transformations and simplicity of the transmission term, the GMS-parameters (4) are ideally suitable for such tasks**. No computational models of probes or launches are required. The GMS-matrix (4) be easily computed or extracted from S-parameters measured for two segments of transmission line with different lengths [24]. Initially we assume that all additional losses and increase in group delay observed originally on Fig. 10 and 11 are attributed to the roughness. According to [19], the roughness correction coefficients can account for the increase in insertion loss, but cannot adjust the group delay as much as we observed in the experiment. The capacitive effect of roughness [18], [19] is practically frequency-independent and cannot be accounted for by any adjustments of the conductor surface impedance discussed in the previous chapter.

We account for this in two different ways; the first and common way is to increase the dielectric constant to match phase or group delay of GMS-parameters as was discussed during the preliminary analysis of measured data. Fig. 16 illustrates this approach for the1080 laminates. Good agreement between measured and computed group delays is due to the correction factor applied to the dielectric constants from original 3 to 3.15 for prepreg to 3.35 for core 1080 laminate, from 3.3 to 3.36 for 2116 prepreg and to 3.25 for 2116 core. An alternative way to account for the additional capacitance is to add spikes or needles to the computational model as illustrated in Fig. 17. This model is more complicated, but it captures the physics of the effect (singularities and additional charges at the sharp peaks). **In this paper we will proceed with the models with adjusted Dk.**
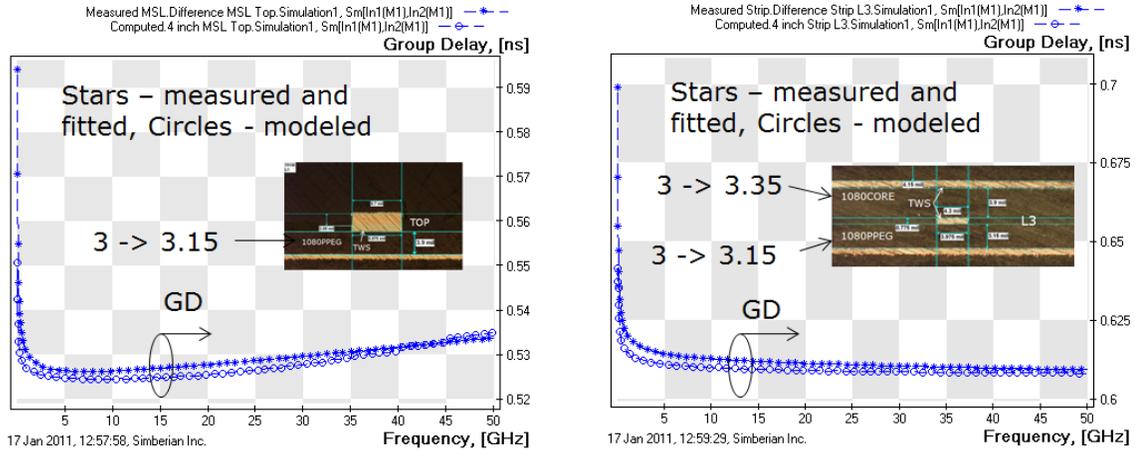
Fig. 16. Measured (stars) and computed with adjusted Dk (circles) generalized modal group delays (GD) of 4 inch microstrip line in top layer (left plot) and strip line in layer L3 (right plot). Foil RTF, laminate 1080.
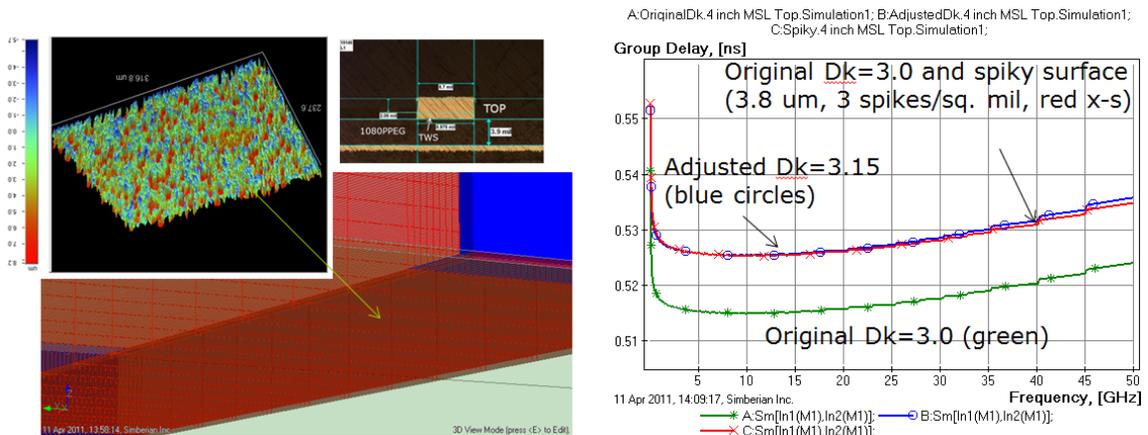

Fig. 17. Possible way to simulate capacitive effect of roughness – add spikes to rough surface of microstrip line. Size and number of spikes are adjusted to match measured group delay.

To simulate the additional losses due to the roughness effect, we will use model (4), similar fitted model from the Simbeor software, and Huray's snowball model [7]. MHCC and Simbeor model have two parameters: Δ and *RF*. If Δ is equal to RMS peak-to-valley (Rq) as in the original HCC model, it can be measured with a profilometer. *RF* can also be mechanically measured as the average increase in path along the rough surface as compared to a flat surface. We used profilometer measurements and computed Rq and RF for two types of foil used on the test board: Rq=2.6 μm, RF=1.85 for RTF foil; Rq=0.68 μm, RF=1.3 for VLP copper. Using this data, the computed insertion loss was larger than measured at lower frequencies and smaller at high frequencies for microstrip in the top layer and stripline in layer L3 made of RTF foil with both MHCC (4) and with the Simbeor model as illustrated in Fig. 18. Insertion loss was substantially lower at all frequencies for a microstrip at the bottom layer and for a strip line in layer L6 made of VLP foil as illustrated in Fig. 19. Huray's snowball model parameters cannot be

computed from the profilometer measurements mainly because the minimum of three parameters required for the model can only be defined if detailed micro-photographs of the surface are available. We did not have access to equipment able to perform computations with Huray's model defined from the physical structure of the surface.
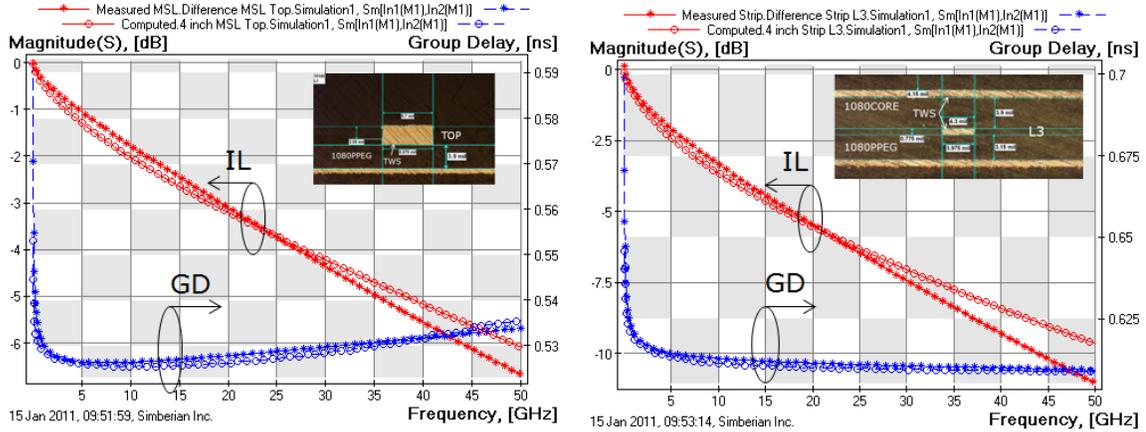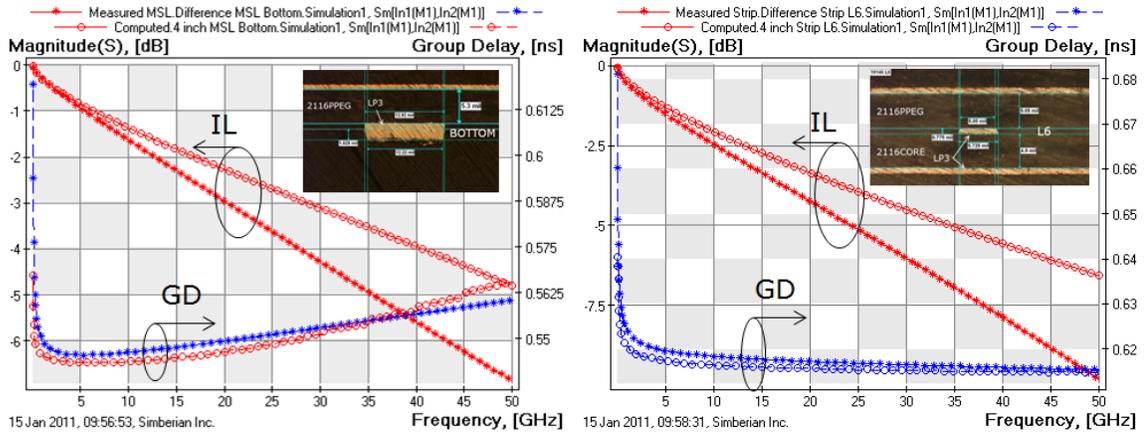

Fig. 18. Measured (stars) and computed (circles) generalized modal insertion loss (IL) and group delay (GD) of 4 inch microstrip line in top layer (left plot) and strip line in layer L3 (right plot). Foil RTF, laminate 1080, Dk of laminates are adjusted, roughness model parameters are measured with profilometer (Rq=2.6 um, RF=1.85).

Fig. 19. Measured (stars) and computed (circles) generalized modal insertion loss (IL) and group delay (GD) of 4 inch microstrip line in bottom layer (left plot) and strip line in layer L6 (right plot). Foil VLP, laminate 2116, Dk of laminates are adjusted, roughness model parameters are measured with profilometer (Rq=0.68 um, RF=1.3).

The mechanical characterization attempt was clearly not successful, especially for low-profile roughness and the reasons have to be further investigated. It may be explained by insufficient resolution of the profilometer or no correspondence in the roughness model parameters with the parameters deduced from the surface geometry. **Thus, we decided to use the roughness correction coefficients and simply optimize the roughness model parameters to achieve good correspondence with the original measured data (minimize the least square error between measured and simulated GMS-parameters).** This procedure was more successful. With $\Delta = 0.35$ and RF=2.8 used

for all surfaces, insertion losses for both microstrip and strip lines made of RTF copper provided a good match to the measured data as shown in Fig. 20 for the Simbeor model. The MHCC model also provided acceptable match with parameters $\Delta = 0.35$ and RF=2.6 as shown in Fig. 21. The least square error between measured and computed generalized magnitude and angle was 0.032 for the Simbeor model, and 0.027 for the MHCC model for the microstrip structure (differences in insertion loss are within 2%).
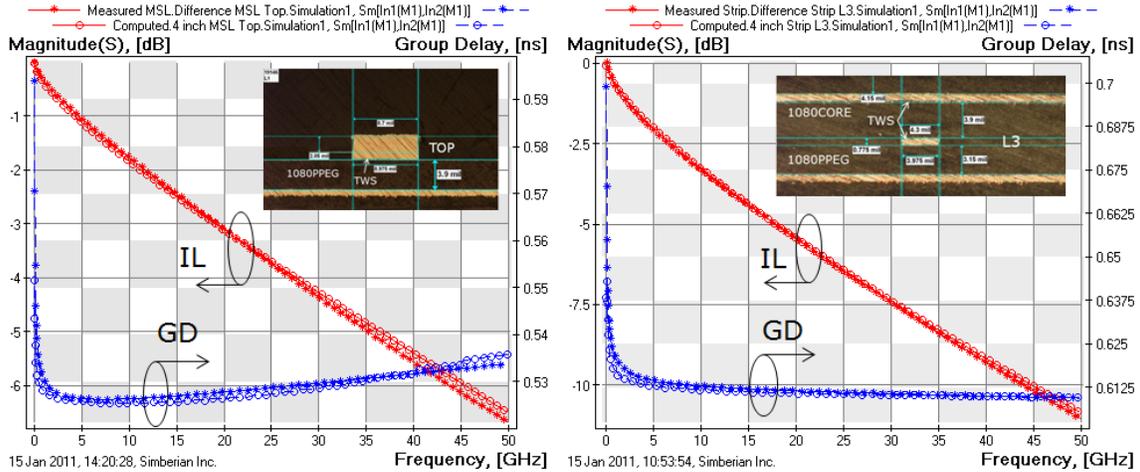

Fig. 20. Measured (stars) and modelled (circles, Simbeor roughness model) insertion loss (IL, red curves) and group delay (GD, blue curves) of 4 inch microstrip line in top layer (left) and strip line in layer L3 (right). Foil RTF, laminate 1080, adjusted Dk, $\Delta = 0.35$ and RF=2.8.
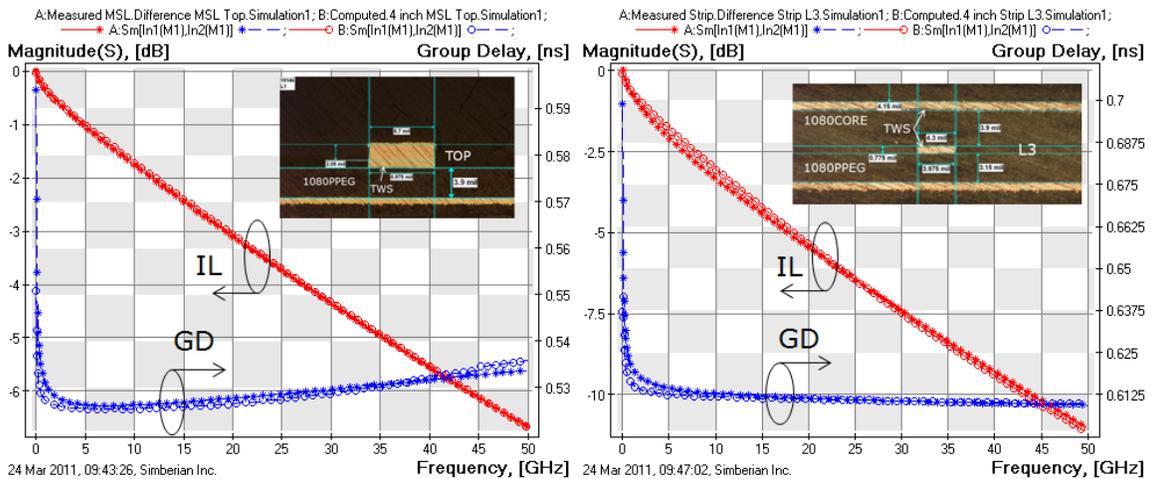

Fig. 21. Measured (stars) and modelled (circles, MHCC roughness model) insertion loss (IL, red curves) and group delay (GD, blue curves) of 4 inch microstrip line in top layer (left) and strip line in layer L3. Foil RTF, laminate 1080, adjusted Dk, $\Delta = 0.35$ and RF=2.6.

Note that the same roughness model is used for the microstrip and for the strip line configurations and in both cases we can conclude that both models provide acceptable accuracy up to 50 GHz. To extract the model parameters we defined the surface roughness and roughness factor as variables, and used optimization to minimize the least square difference between measured and computed GMS-parameters. Note also, that if we add relative copper resistivity as a parameter (Rr), the optimization produces slightly different parameters with about the same value of least square error. For instance, for the Simbeor model we have $\Delta = 0.45$ and RF=2.4 and Rr=1.11. A combination of $\Delta = 0.4$ and RF=2.4 and Rr=1.1 in MHCC also produces good match with about the same value of least square error. We can achieve a better match at DC by including the resistivity parameter. The non-uniqueness of parameters is definitely a disadvantage of such an approach, though it is perfectly suitable for practical applications as long as it provides good correspondence for a set of micro-strip and strip-line structures on the same board.

There are more parameters to match Huray's snowball model as shown in [7] – the minimal number of parameters is three (in addition to the resistivity of copper): ball radius, base tile size and number of balls. Technically, the number of balls and tile area size may be considered as one parameter in the formula provided in [7], in order to reduce the number of parameters for optimization. Thus, we fixed the number of balls to 15 and optimized the other two parameters to minimize the least square error – the results are illustrated in Fig. 22. The least square error in this case is 0.033 that is comparable with the cases of the Simbeor and MHCC models. The efforts of some vendors in microscopic characterization of copper surfaces with the parameters for Huray's model may eventually make this model more practical.
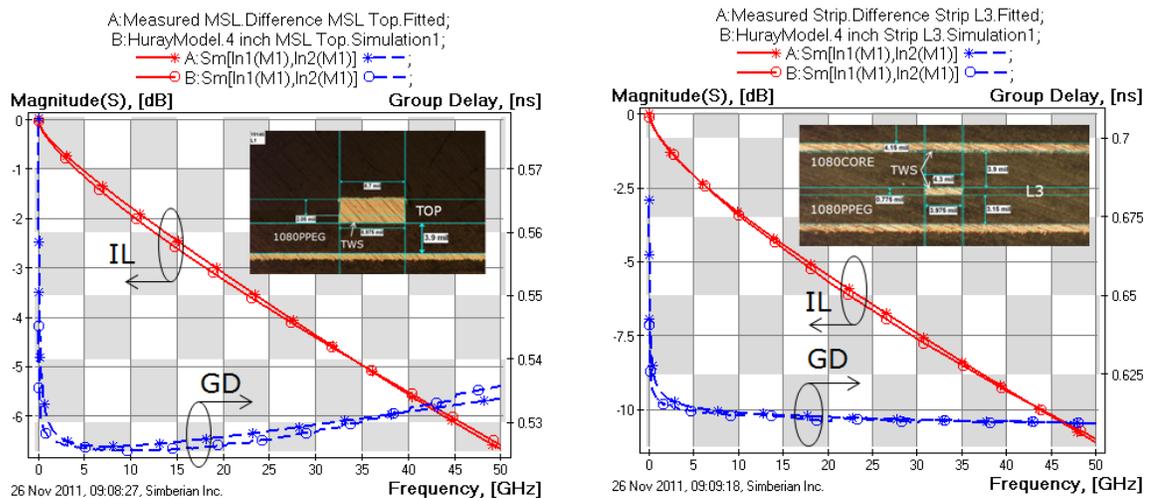

Fig. 22. Measured (stars) and modelled (circles, Huray's snowball roughness model) insertion loss (IL, red curves) and group delay (GD, blue curves) of 4 inch microstrip line in top layer (left) and strip line in layer L3. Foil RTF, laminate 1080, adjusted Dk, ball radius 0.5 um, tile size 4.98 um, Nb=15.

Finally, in order to match the measured and simulated insertion loss for microstrip in bottom layer and strip line in layer L6 (VLP foil) we have adjusted the roughness parameters in Simbeor model as follows: $\Delta = 0.11$ and RF=7. The dielectric constant

adjustment for 2116 laminate with VLP copper foil was relatively small: from 3.3 to 3.36 for prepreg and to 3.25 for core layers. The results are illustrated in Fig. 23 for Simbeor model (similar results are obtained with the MHCC model). VLP foil showed smaller loss increase at lower frequencies (thus smaller Δ), but larger increase with the frequency (larger roughness factor *RF*). It also showed smaller increase in the capacitance due to absence of sharp spikes on this type of treated foil. The match in this case was not ideal (least square error 0.054). We can also notice from Fig. 23 that if the roughness model is identified with the microstrip structure, there are growing discrepancies in the generalized insertion loss for the strip line in layer L6. The reason for these discrepancies need to be investigated further. Overall, the model can be considered acceptable for the practical analysis of both microstrip and stripline structures with VLP foil up to 40 GHz.
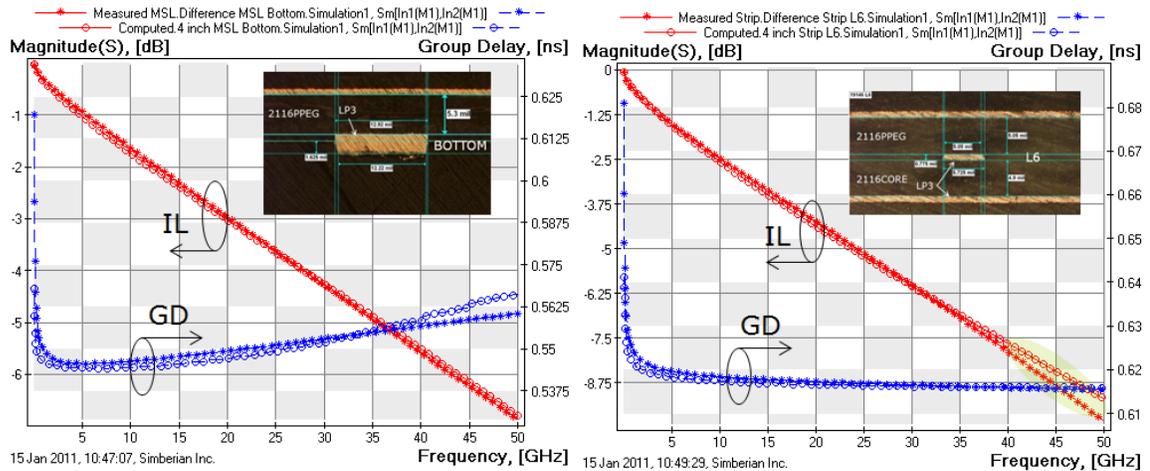

Fig. 23. Measured (stars) and modelled (circles, Simbeor roughness model) insertion loss (IL, red curves) and group delay (GD, blue curves) of 4 inch microstrip line in top layer (left) and strip line in layer L3 (right). Foil VLP, laminate 2116, adjusted Dk, $\Delta = 0.11$ and RF=7.

In summary, we have shown the possibility to achieve good accuracy in modelling rough interconnects with surface impedance roughness correction coefficients. Parameters of the correction coefficients can be defined by matching measured and modelled generalized modal insertion loss and group or phase delay for line segments. One roughness model has been used for strip and microstrip lines made of the same foil within the same dielectric and with different strip widths.

6. Conclusion

The main result of this paper is a simple and practical methodology for characterization and identification of the conductor roughness effect on signal propagation in interconnects. Conductor differential surface impedance operator is constructed with Trefftz finite elements and locally adjusted with a roughness correction coefficient. Practically any roughness correction coefficient derived for the roughness characterization can be used with this approach. Hammerstad correction coefficient is modified with a roughness factor to account for variations in maximal possible increase in attenuation due to roughness. The roughness model parameters were identified with

the generalized modal S-parameters. It was shown that the suggested approach is acceptable for analysis of interconnects on such a board within some variation of trace widths at frequencies from DC to 50 GHz or with data rates up to 25-30 Gbps. It was also shown that using roughness correction coefficients can provide comparable accuracy in analysis of additional losses due to roughness. Substantial increase of effective dielectric constant due to conductor surface roughness has been observed and explained by capacitive effect of nearly singular spikes on the surface of conductor.

There remains a lot of uncertainties in modeling of interconnects on PCBs. Effects like inhomogeneity of dielectrics, weave effect, relatively large variations of dimensions and roughness make accurate analysis of interconnects on PCBs extremely difficult. This paper reports work in progress; in order to further investigate roughness, we are building another set of test boards with different foils and more homogeneous I-Tera resin-systsem using 3313, 1067 or 1086 weave.

Acknowledgements

References

[1] S.P. Morgan Jr., "Effect of Surface Roughness on Eddy Current Losses at Microwave Frequencies," *Journal of Applied Physics*, Vol. 20, p. 352-362, April, 1949.

[2] E.O. Hammerstad, F. Bekkadal, *Microstrip Handbook*, Univ. Trondheim., 1975.

[3] E.O. Hammerstad, Ø. Jensen, "Accurate Models for Microstrip Computer Aided Design", *IEEE MTT-S Int. Microwave Symp. Dig.*, p. 407-409, May 1980.

[4] G. Brist, S. Hall, S. Clouser, T. Liang, "Non-classical conductor losses due to copper foil roughness and treatment," *2005 IPC Electronic Circuits World Convention,* February 2005.

[5] T. Liang, S. Hall, H. Heck, & G. Brist, "A practical method for modeling PCB transmission lines with conductor roughness and wideband dielectric properties," IEE MTT-S Symposium Digest, p. 1780, November 2006.

[6] S. Hall, S. G. Pytel*,* P. G. Huray*,* D. Hua, A. Moonshiram*,* G. A. Brist, E. Sijercic, "Multigigahertz Causal Transmission Line Modeling Methodology Using a 3-D Hemispherical Surface Roughness Approach", *IEEE Trans. On MTT*, vol. 55, No. 12, p. 2614-2623, Dec. 2007.

[7] P. G. Huray, O. Oluwafemi, J. Loyer, E. Bogatin, X. Ye "Impact of Copper Surface Texture on Loss: A Model that Works", *DesignCon 2010.*

[8] A.F. Horn, J.W. Reynolds, J.C. Rautio, "Conductor profile effects on the propagation constant of microstrip transmission lines", 2010 IEEE MTT-S International Microwave Symposium Digest (MTT), May 2010. p. 868 – 871.

[9] S. Sandstroem, "Stripline Models with Conductor Surface Roughness", *Master of Science Thesis*, Helsinki University of Technology, Finland, February 2004.

[10] S. Hinaga, M., Koledintseva, P. K. Reddy Anmula, & J. L Drewniak, "Effect of conductor surface roughness upon measured loss and extracted values of PCB laminate material dissipation factor," *IPC APEX Expo 2009 Conference*, Las Vegas, March 2009.

[11] L. Tsang, X. Gu, & H. Braunisch, "Effects of random rough surfaces on absorption by conductors at microwave frequencies, *IEEE Microwave and Wireless Components Letters,* v. 16, n. 4, p. 221, April 2006.

[12] R. Ding, L. Tsang, & H. Braunisch, "Wave propagation in a randomly rough parallel-plate waveguide," *IEEE Transactions on Microwave Theory and Techniques,* v. 57, n.5, May 2009.

[13] Deutsch, A. Huber, G.V. Kopcsay, B. J. Rubin, R. Hemedinger, D. Carey, W. Becker, T Winkel, B. Chamberlin, "Accuracy of Dielectric Constant Measurement Using the Full-Sheet-Resonance Technique IPC-T650 2.5.5.6 " p. 311-314, *., IEEE Symposium on Electrical Performance of Electronic Packaging,* 2002.

[14] X. Chen, "EM modeling of microstrip conductor losses including surface roughness effect," *IEEE Microwave and Wireless Components Letters,* v. 17, n.2, p. 94, February 2007.

[15] C. L. Holloway*,* E. F. Kuester, "Impedance-Type Boundary Conditions for a Periodic Interface Between a Dielectric and a Highly Conducting Medium", *IEEE Trans. on AP*, vol. 48, N 10, p. 1660-1672, Oct. 2000.

[16] M. V. Lukic´*,* D. S. Filipovic*,*"Modeling of 3-D Surface Roughness Effects With Application to -Coaxial Lines", IEEE Trans. on MTT, vol. 55, No. 3, p. 518-525, 2007.

[17] D. L. Jaggard, "On fractal electrodynamics," in *Recent Advances in Electromagnetic Theory*,H.N. Kritikos and D. L. Jaggard, Eds. Berlin, Germany: Springer-Verlag, ch. 6, p. 183–224, 1990.

[18] A. Albina at al., Impact of the surface roughness on the electrical capacitance, Microelectronics Journal, v. 37, 2006, p. 752–758.

[19] Y. Shlepnev, C. Nwachukwu, "Roughness characterization for interconnect analysis". - Proc. of the 2011 IEEE International Symposium on Electromagnetic Compatibility, Long Beach, CA, USA, August, 2011, p. 518-523.

[20] M. Koledintseva, A. Koul, F. Zhou, J. Drewniak, and S. Hinaga, Surface Impedance Approach to Calculate Loss in Rough Conductor Coated with Dielectric Layer, Proc. of the 2010 IEEE International Symposium on Electromagnetic Compatibility, Fort Lauderdale, FL, USA, July, 2010, p. 790-795.

[21] A.B. Bereskin, "Microwave Dielectric Property Measurements", *Microwave Journal*, v. 35, no. 7, pp 98-112., 1992.

[22] Simbeor Electromagnetic Signal Integrity Software, www.simberian.com

[23] Djordjevic, R.M. Biljic, V.D. Likar-Smiljanic, T.K.Sarkar, Wideband frequency domain characterization of FR-4 and time-domain causality, IEEE Trans. on EMC, vol. 43, N4, 2001, p. 662-667.

[24] Y. Shlepnev, A. Neves, T. Dagostino, S. McMorrow, "Practical identification of dispersive dielectric models with generalized modal S-parameters for analysis of interconnects in 6-100 Gb/s applications", in Proc. of *DesignCon* 2010.

[25] Y. Shlepnev, "The System and method for identification of complex permittivity of transmission line dielectric" Patent pending #61/296,237.

[26] Y. Shlepnev, S. McMorrow, "Nickel characterization for interconnect analysis, ". - Proc. of the 2011 IEEE International Symposium on Electromagnetic Compatibility, Long Beach, CA, USA, August, 2011, p. 524-529.

[27] Y.O. Shlepnev, "Extension of the Method of Lines for planar 3D structures", in *Proceedings of the 15th Annual Review of Progress in Applied Computational Electromagnetics (ACES'99)*, Monterey, CA, p.116-121, 1999.

[28] Y.O. Shlepnev, "Trefftz Finite Elements for Electromagnetics", *IEEE Trans. Microwave Theory Tech.*, vol. MTT-50, pp. 1328-1339, May, 2002.

[29] Y. O. Shlepnev, B. V. Sestroretzkiy, V. Y. Kustov, "A New Approach to Modeling Arbitrary Transmission Lines", *Journal of Communications Technology and Electronics,* v. 42, N 1, p. 13-16, 1997.

[30] D. De Zutter*,* L. Knockaert, "Skin Effect Modeling Based on a Differential Surface Admittance Operator", *IEEE Trans. on MTT*, vol. 53, N 8, p. 2526-2538, 2005.

[31] H.A. Wheeler, "Transmission Line Properties of Parallel Strips Separated by a Dielectric Sheet", *IEEE Trans. on MTT*, vol. 13, p. 72-185, March 1965.

[32] Romo, Gerardo. et. al., "Stack-Up and Routing Optimization by Understanding Micro-Scale PCB Effects." DesignCon 2011